The influence of measurement uncertainties on the evaluation of the distribution volume ratio in rat studies on a microPET® R4: a phantom study

V Sossi, *Member, IEEE* M-L Camborde, D Newport, *Member, IEEE,* A Rahmim, *Member, IEEE,* G Tropini, DJ Doudet, TJ Ruth

***Abstract*—In small animal imaging the injectable radiotracer dose is often limited by the tracer mass effect. Biological considerations as opposed to the count rate capabilities of the scanner are thus often the limiting factor for the maximum allowed radiotracer dose, which in turn, together with the tracer kinetics and scanner sensitivity, dictates the statistical quality of the time activity curves (TACs) used to extract biologically significant parameters. We investigated the effect of measurement uncertainty on the determination of the distribution volume ratio (DVR) and binding potential (BP) as estimated using the tissue input Logan (DVR_L, BP_L) and the ratio (DVR_r, BP_r) methods for two different tracers, with the Concorde microPET® R4 camera. TAC templates extracted from rat studies and phantom data were used. We found that for a tracer with relatively fast kinetics, ^{11}C-dihydrotetrabenazine (DTBZ), the overall coefficient of variation (COV) was 11% for the BP_L and 13.4% for the BP_r, when the BP was calculated using TACs obtained from individual regions of interest (ROIs). The COVs were reduced to 7.5% (BP_L) and 8.6% (BP_r) when the striatal and cerebellar TACs were estimated as averages of 3 and 2 ROIs respectively. Similar results obtained for a tracer with slower kinetics ^{11}C-methylphenidate (MP), yielded approximately 30% higher COVs. The above values were obtained when segmented attenuation correction was applied to the data; with measured attenuation correction the COVs were on average 50% higher.**

I. Introduction

THE radiotracer dose in neuroreceptor imaging is limited by the requirement that the tracer amount should not occupy more than 1% of the available receptors [1]. This requirement is particularly significant in small animal studies: due to their minute size, the maximum amount of radiotracer that can be administered without inducing significant receptor occupancy, results in count rates that are generally well below the count rate capabilities of the cameras. Likewise, the acquisition time for each frame is generally limited by the need of capturing the changes of the radiotracer distribution as a function of time in sufficient detail to permit an accurate biologically relevant analysis. These two requirements cause the number of acquired counts for each time frame to be often quite low, thus raising the question about the influence of the statistical quality of the acquired data on the variability of the final biological parameter. Inaccurate quantification corrections are additional possible sources of uncertainty, since they lead to artificial image non-uniformities. For example, attenuation correction factors derived directly from a transmission scan (measured attenuation correction) have been identified as a definite contributor to uniformity degradation [2]. As the imaging protocols and the biological questions being asked become increasingly more complex, thus requiring an increased precision in the evaluation of specific parameter values, it becomes more and more relevant to determine the accuracy limitations due to the statistical and instrumentation-related quality of the data. It must be however noticed that such determination provides only a lower limit to the accuracy of the parameter evaluation, since in-vivo measurement reproducibility is also influenced by biological variability, which is not addressed in this study.

There are often several methods that can be used to provide estimates of specific biologically relevant parameters. For example, an estimate of the binding potential (BP), which is the most commonly used parameter to quantify binding of reversible tracers, can be obtained using compartmental models [3-5], simple ratio estimates [6] or graphical methods [7-8]. Each of this methods may use a different combination of the acquired data: for example, ratio methods often use tracer distribution values averaged over relatively long times (of the order of 30 minutes), compartmental models use data acquired within each time frame, while graphical methods typically use a combination of time-averaged (or time-integrated) data and values from single time frames. Each of these methods is thus differently sensitive to the statistical noise of the data. In our evaluation we considered two methods used to obtain estimates

This work was supported by a TRIUMF Life Science grant, by the National Sciences and Engineering Research Council of Canada (VS and AR) and by the Michael Smith Foundation for Health and Research (VS).

V.S. is with the University of British Columbia, Vancouver, B.C., Canada, V6T 1Z1 (telephone 604 822 7710, e-mail vesna@phsyics.ubc.ca)

M-L. C is with TRIUMF, Vancouver B.C., Canada V6T 2A3 (e-mail marie@pet.ubc.ca)

D.N. is with CTI, Knoxville, TN, USA, e-mail dnewport@cms-asic.com

A.R. is with the University of British Columbia, Vancouver, B.C., Canada V6T 1Z1 (e-mail rahmim@physics.ubc.ca)

GT is with the University of British Columbia, Vancouver, B.C., Canada, V6T 1Z1 (e-mail giorgia@pet.ubc.ca)

DD is with the University of British Columbia, Vancouver, B.C, Canada V6T 1B5 (e-mail ddoudet@interchange.ubc.ca) CHECK POSTAL CODE

TJR is with TRIUMF, Vancouver B.C., Canada V6T 2A3 (e-mail truth@triumf.ca)

of the BP: the tissue input Logan graphical approach (BP_L) [8], and the simple target to reference region ratio (BP_r). In all these methods the directly determined variable is the tracer distribution volume ratio (DVR_L, DVR_r), which is generally related to the BP as DVR = BP+1. Only blood-less methods were considered, since in small animal scanning blood sampling is not easily feasible.

In order to achieve an evaluation of the impact of the statistical and instrumentation-related quality of the data on the final parameter determination, it is necessary to create reproducible scanning conditions, where the results differ only because of the statistical variation of the radioactivity concentration measurement and possibly because of the location of the region of interest in the scanner field of view and thus in the image. To obtain these conditions we have created replicas of time activity curves (TACs) representative of those obtained in typical rat ^{11}C-dyhidrotetrabenazine (DTBZ – a monoamine vesicular transporter VMAT2 marker) and ^{11}C-methylphenidate (MP – a dopamine membrane transporter DAT marker) studies by extracting appropriate time frames from a dynamic study of a phantom filled with a uniform radioactivity concentration('rat phantom'). By placing several identical ROIs on the 'rat-phantom', several realizations of the TACs were obtained. For each TAC we calculated estimates of the tracer DVR_L, DVR_r and BP_L and BP_r and eventually their coefficients of variation. The analysis was performed for two tracers, since the outcome is dependent on the relative tracer accumulation in the target and reference regions, which varies for different tracers, as well as tracer kinetics. Simulation studies by Meikle et al. [9] in-fact showed that the BP of tracers with slower kinetics is more susceptible to a low statistical quality of the data compared to tracers with faster kinetics.

Since measured attenuation had been identified as a significant source of instrumentation-related inaccuracy the analysis was performed on rat and phantom data reconstructed with measured attenuation correction factors and attenuation correction factors obtained after appropriately segmenting the attenuation maps into pre-defined μ-values.

Given a certain injected dose, the number of acquired counts depends mostly on the scanner sensitivity (assuming, as mentioned earlier, that the count rates are well below the count rate capabilities of the scanner). The results presented here are thus valid for the specific scanner used, the Concorde microPET® R4 [10], which has an absolute sensitivity of approximately 2%. The methodological procedure presented in this paper is however, directly applicable to any scanner.

II. METHODS

Rat studies. Data from two MP and two DTBZ studies on the same rat were used to obtain the TACs which served as templates when forming TACs from the phantom study. In all cases rats were injected with 100μCi/100g of tracer with sufficiently high specific activity to satisfy the tracer principle requirement. Each study consisted of a 10 min transmission scan, followed by 6 x 30sec, 2 x 60sec, 5 x300sec, 2 x 450 and 2 x 480 sec of emission data for a total of 60 min. Images were reconstructed with all corrections except for decay, using Fourier rebinning and FBP. Separate reconstructions were performed for segmented and measured attenuation correction. For the purpose of this study the striatal TAC was obtained from the average of six striatal 6.4 mm^2 regions of interest ROIs (placed on the left and right striatal image on three consecutive axial planes). The reference region template TAC was obtained from two 20 mm^2 ROIs placed on the cerebellar region (one on each contiguous axial plane) which is typically located approximately 11 axial planes (1.2 cm) away from the striatum. The ROIs were taken from a template which is commonly used in our centre. During our standard analysis of the rat data a separate TAC is formed for each striatum by averaging the values of the ROIs on the three axial planes.

Phantom studies –choice of phantom. The TACs used in the Logan and ratio analyses are obtained from PET data that are fully corrected except for the overall sensitivity calibration (conversion from count density to concentration). Such corrections, for example attenuation and scatter corrections, alter the final image intensity values. The magnitude of these correction factors depends on the density and size of the object being scanned. It was thus important that the size and density of the phantom used in this study closely resembles the size and density of a rat. We found that a 2.5cm diameter cylinder filled with an aqueous radioactivity concentration provided a good match. The accuracy of the match was verified by ensuring that the ratio between image intensity values of a ROI centrally placed on the scatter and attenuation corrected image and the same ROI placed on the uncorrected image was very similar for both for the phantom and the rat studies. We could thus assume that the same image intensity values observed in the scatter and attenuation corrected phantom and rat study would be representative of the same number of acquired counts/voxel and thus total acquired counts for the same scan duration. The 2.5 cm diameter cylinder will be here-after referred to as 'rat phantom'.

Phantom studies – scans performed. The 'rat phantom' was filled with an aqueous solution containing 35.4 MBq of ^{11}C and scanned for 3 hours, covering a count rate range from 268.6 x 10^3 cnts/sec to 0.67 x 10^3 cnts/sec. The cylinder was placed into the rat head holder and positioned asymmetrically in the axial direction to simulate as close as possible the rat scanning conditions, including contributions from radioactivity from outside the field of view (FOV). List mode acquired data were binned into 30 sec intervals and reconstructed with all corrections except for decay using Fourier rebinning and FBP. As for the rat studies, data were reconstructed separately with measured and segmented attenuation correction.

Formation of phantom TACs. 'rat-phantom' data sets were extracted from the phantom study by selecting those frames where the measured concentration in the phantom study

matched that in a selected rat TAC. The average over all planes of the phantom study was used to define the appropriate 'rat-phantom' data sets so as to avoid possible inconsistencies due potential local non-uniformities in the phantom image. In order to match for the frame duration of the rat studies and consequently the number of acquired counts per frame, the appropriate number of 30 sec frames of the phantom data was added together (appropriately centered around the identified matching 30 sec frame). The result was thus a unique 17 frame subset of the entire phantom data set for each rat TAC.

Once the appropriate dynamic sequence of phantom images was formed, ROIs of the same size as those used in the rat image analysis were placed on the phantom image. 66 striatal size (9 pixels) and 60 cerebellar size (28 pixels) ROIs were placed across several axial planes. Since these ROIs were placed on images of a uniform phantom, the only difference between them was assumed to be of statistical nature with a possible contribution from intrinsic image non-uniformities. Once the TACs were formed as described, the appropriate decay corrections relative to the rat data framing sequence (see Rat studies) were applied to replicate the TACs required by the Logan analysis.

Image analysis and statistical analysis of results. The effect of measurement uncertainty was evaluated for four parameters BP_L, BP_r, DVR_L and DVR_r. Since these parameters are often calculated on TACs obtained as averages from single ROI TACs (see Rat studies), we investigated the variation of the parameter coefficients of variation as a function of ROI averaging. The parameters estimates were thus calculated for the conditions described in table 1. Str3_Cer2 is the method that effectively corresponds to that used in the standard analysis of the rat data in our centre.

TABLE I
FORMATION OF THE TACS USED IN THE EVALUATION OF THE FOUR PARAMETERS

Method	Striatal TAC (number of TACs)	Cerebellar TAC (number of TACs)	Total number of estimates
Str_Cer_Ind	Individual (66)	Individual (60)	3960
Str_2	Average over 2 ROIs (33)	Individual (60)	1980
Str_3	Average over 3 ROIs (22)	Individual(60)	1320
Cer_2	Individual (66)	Average over 2 ROIs (30)	1980
Cer_3	Individual (66)	Average over 3 ROIs (20)	1320
Str2_Cer2	Average over 2 ROIs (33)	Average over 2 ROIs (30)	990
Str3_Cer2	Average over 3 ROIs (22)	Average over 2 ROIs (30)	660

The figure of merit used to describe the statistical accuracy of the data was the coefficient of variation (COV). An overall coefficient of variation (COV_o) was calculated for each method by estimating the mean and standard deviation of each parameter obtained with each striatal and cerebellar TAC combination. In addition, we separated the contribution of the striatal and cerebellar data to the overall COV. To determine the COV due to the striatal TACs, the COV amongst the parameter values was calculated for each cerebellar TAC separately (that is keeping the same cerebellar TAC and varying the striatal TAC) and the resulting COV samples were averaged to produce the 'striatal COV' (COV_s). Likewise to determine the COV due to the cerebellar TACs, the COV was calculated for each striatal TAC separately (that is keeping the striatal TAC the same and varying the cerebellar TAC) and the resulting COV samples were averaged to produce the 'cerebellar COV' (COV_c). This analysis was performed for each rat TAC template. The presented results are averages over two rat templates for each tracer.

III. RESULTS

Rat and 'rat phantom' TACs. Figure 1 shows the TACs obtained from one of the MP and one of the DTBZ rat scans. The difference in their kinetic behavior is clearly visible.

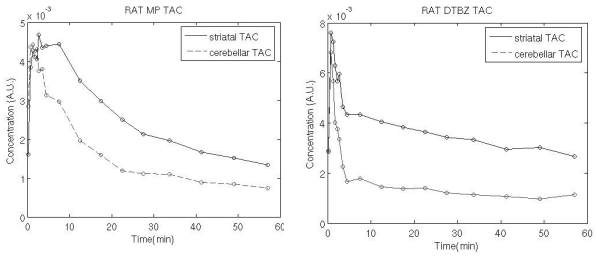

Figure 1.TACs from an MP and a DTBZ rat scan.

Figure 2 shows a comparison between striatal and cerebellar TACs obtained from rat studies and the corresponding ones formed from the rat phantom using plane averages (see methods). Very good agreement is observed. Figure 3 shows an example of the replicas of the same TAC obtained from the 'rat phantom'data.

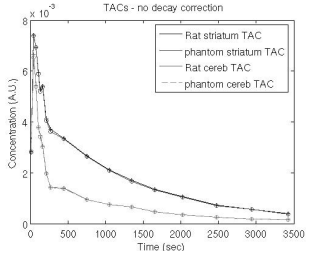

Figure 2. Comparison between the rat and 'rat phantom' TACs obtained from plane averages. The corresponding TACs are essentially overlaid.

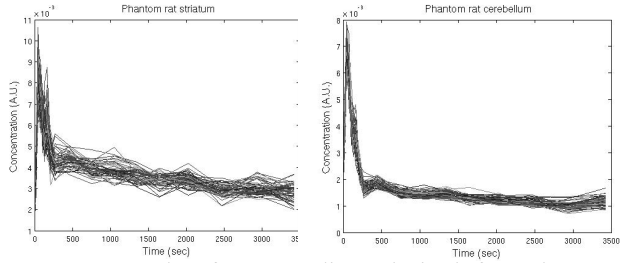

Figure 3. Example of TAC replicas obtained from the 'rat phantom' data.

COV analysis. The results of the COV analysis for the segmented attenuation corrected data are presented in figures 4-7, while a subset of equivalent results obtained for measured attenuation corrected data is shown in figure 8.

IV. Discussion

The effect of several factors can be determined from an analysis of the data presented in figures 4-8.

Accuracy of attenuation correction effect. A comparison of the data in figures 4 and 8 clearly shows that the measured attenuation correction introduces significant non-uniformities into the images as confirmed by other studies [2]. The discussion will thus be focused onto the results obtained with segmented attenuation corrected data. Thus all figures, except figure 5 shows results from data processed with segmented attenuation correction.

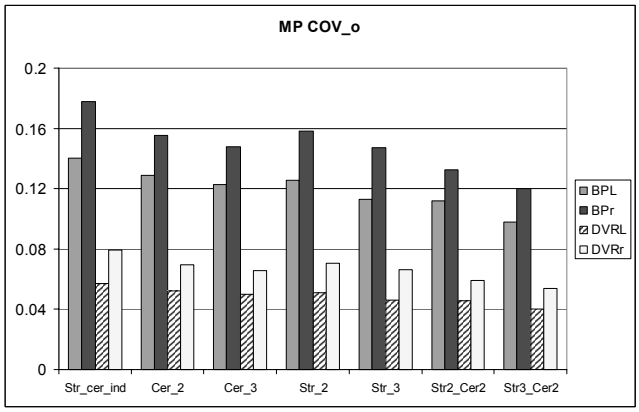

Figure 4. COV_o for the TAC configurations listed in table 1 for all four parameters for MP.

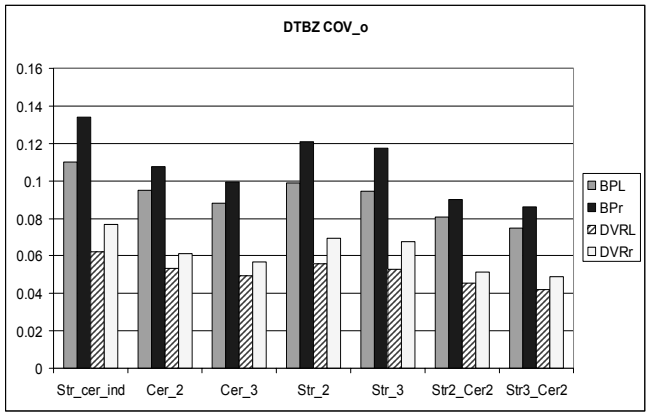

Figure 5. COV_o for the TAC configurations listed in table 1 for all four parameters for DTBZ.

Tracer effect. In agreement with the results of Meikle et al. [9] a greater COV was observed for MP, the tracer with slower kinetic. For the BP measures, for DTBZ the largest COV was 13.4%, while for the MP the largest COV was 17.8%. For the DVR measures, the corresponding values were 7.7% and. 7.9%

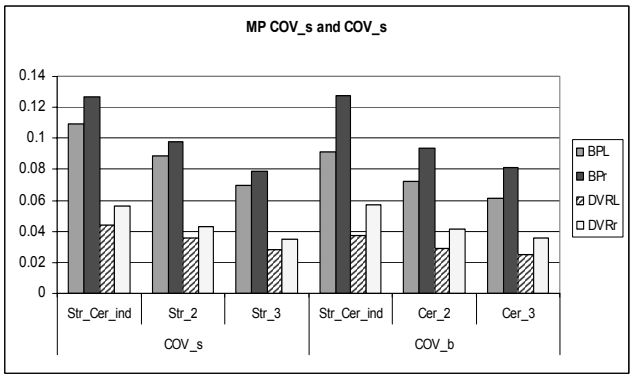

Figure 6. COV_s and COV_c for the TAC configurations listed in table 1 for all four parameters for MP.

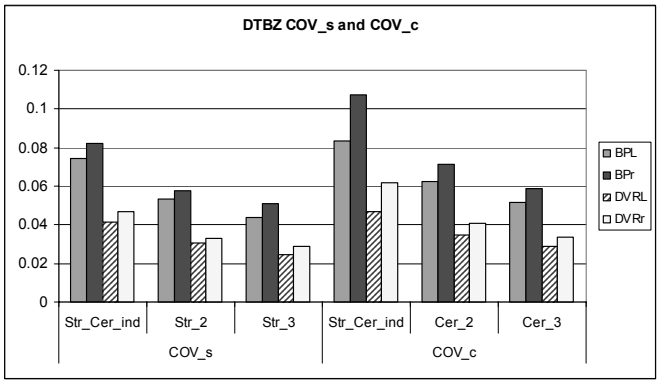

Figure 7. COV_s and COV_c for the TAC configurations listed in table 1 for all four parameters for MP for DTBZ.

Region of interest effect. For MP the total COV has similar contribution from the variability of the striatal and the cerebellar region, while for DTBZ the COV of the cerebellar regions seems to contribute slightly more to the overall COV compared to COV_s. The similarity of the two contributions can be explained by the fact that the radiotracer concentration is higher in the striatum, however the ROI placed on the cerebellar region is larger, thus reducing the statistical noise. In all cases averaging concentration values over several ROIs noticeably reduces the COV. In the extreme case tested (striatal TAC averaged over 3 ROIs and cerebellar TAC averaged over 2 cerebellar ROIs) the COV drops to below approximately 8.6 % for DTBZ and 12% for MP for the BP measures and below 5% and 5.4% respectively for the DVR measures. Due to the limited size of the rat brain, further averaging was not considered realistic.

Analysis method effect. Interestingly the parameters determined with the Logan graphical approach appear more robust with respect to measurement uncertainties compared to those obtained with simple ratio methods, with total COVs that

are generally 20% lower compared to those for the equivalent parameter estimates obtained with the ratio approach. In particular, the parameter estimates obtained with the ratio methods are much more sensitive to the variability of the cerebellar region (figures 6 and 7). The COV for the DVR estimates is clearly lower compared to that of the BP estimates, since the BP values are derived from the DVR values by subtracting 1. However, although DVR is directly measured, BP has a more relevant biological meaning, since it is more closely related to the tracer binding to the specific sites of interest. The BP COV estimates should thus be considered of primary importance when evaluating the effects of statistical and instrumentation-related inaccuracies on a biologically important outcome of reversible tracer PET studies.

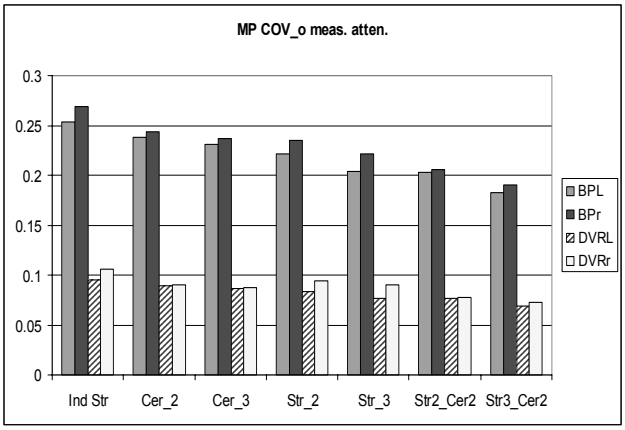

Figure 8. COV_o for the TAC configurations listed in table 1 for all four parameters for measured attenuation. To be compared to data in figure 4.

V. Conclusion

We developed a phantom and rat data based method that allows for the determination of the contribution of the measurement uncertainty to the variability of biological parameters. The method was applied to the data acquired with the microPET® R4 scanner. The analysis showed that measured attenuation correction in this particular scanner introduces noticeably more variability into the final results of the data analysis compared to segmented attenuation. A tracer and analysis method dependent variability was observed in the results, with COVs ranging from approximately 18% to 7.5% for BP estimates and 8% to 4% for the DVR measures. Furthermore, the analysis has confirmed that methods used to extract DVR and BP suffer are differently sensitive to the measurement uncertainties with the graphical method proving more robust compared to the ratio method. The combination of averaging over as many ROIs as feasible and using a graphical approach for parameter determination together with a segmented attenuation correction method have been shown to produce fairly robust BP and DVR estimates at injected doses that to not violate the tracer principle. In addition to providing useful data in the studies presented here, the described method can be used to further explore the effect of data acquisition and processing on the variability of the final, biologically relevant parameters as well as comparing the sensitivity of various parameter extracting methods to statistical and instrumentation-related uncertainties.

VI. Acknowledgement

The authors thank Siobhan McCormick for assistance in data analysis and rat scanning, and Rick Koernelsen and Ivan Cepeda for assistance in rat scanning.

VII. References

[1] Hume SP, Gunn RN, Jones T, Pharmacological constraints associated with positron emission tomographic scanning of small laboratory animals, Eur J Nucl Med. 1998 Feb;25(2):173-6

[2] Camborde ML, Rahmim A, Newport D, Siegel S, Buckley KR, Vandervoort E, Ruth TJ, Sossi V, Effect of normalization method on image uniformity and binding potential estimates on microPET®, Proceedings of the 2004 IEEE/MIC, Rome, Italy

[3] Lammertsma AA, Hume SP, Simplified reference tissue model for PET receptor studies. Neuroimage. 1996 (4): 53-8.

[4] Lammertsma AA, Bench CJ, Hume SP, Osman S, Gunn K, Brooks DJ, Frackowiak RS, Comparison of methods for analysis of clinical [11C]raclopride studies, J Cereb Blood Flow Metab. 1996 16(1):42-52

[5] Gunn RN, Lammertsma AA, Hume SP, Cunningham VJ Parametric imaging of ligand-receptor binding in PET using a simplified reference region model Neuroimage. 1997 Nov;6(4):279-87

[6] Ito H, Hietala J, Blomqvist G, Halldin C, Farde L Comparison of the transient equilibrium and continuous infusion method for quantitative PET analysis of [11C]raclopride binding J Cereb Blood Flow Metab. 1998 18(9):941-50.

[7] Logan J, Fowler JS, Volkow ND, Wolf AP, Dewey SL, Schlyer DJ, MacGregor RR, Hitzemann R, Bendriem B, Gatley SJ, Graphical analysis of reversible radioligand binding from time-activity measurements applied to [N-11C-methyl]-(-)-cocaine PET studies in human subjects J Cereb Blood Flow Metab. 1990 10(5):740-7

[8] Logan J, Fowler JS, Volkow ND, Wang GJ, Ding YS, Alexoff DL, Distribution volume ratios without blood sampling from graphical analysis of PET data, J Cereb Blood Flow Metab. 1996 16(5):834-40

[9] Meikle SR, Eberl S, Fulton RR, Kassiou M, Fulham MJ, The influence of tomograph sensitivity on kinetic parameter estimation in positron emission tomography imaging studies of the rat brain Nucl Med Biol. 2000 7(6):617-25

[10] Knoess C, Siegel S, Smith A et al, Performance evaluation of the microPET R4 PET scanner for rodents Eur J Nucl Med Mol Imaging 2003 Ma30(5):737-47